JTTEE5 21:818–824
DOI: 10.1007/s11666-012-9760-3
1059-9630/$19.00 © ASM International

Mechanical Properties and Thermal Shock Resistance of HVOF Sprayed NiCrAlY Coatings Without and With Nano Ceria

Xiaoguang Sun, Shufen Chen, You Wang, Zhaoyi Pan, and Liang Wang

(Submitted August 31, 2011; in revised form January 2, 2012)

NiCrAlY coatings without and with 0.2 wt.% nano ceria were prepared by high velocity oxygen fuel spraying. The microstructure, mechanical properties, and thermal shock resistance of as-sprayed coatings were investigated. The results showed that in the as-sprayed coatings, the number of un-melted particles was reduced drastically, the microstructure was refined and compact due to the refinement of sprayable powders. Both the hardness and adhesive strength of the NiCrAlY increased due to the refinement of microstructure and the decrease of the defects, such as pores and oxides, after adding nano ceria. The thermal cycle life of NiCrAlY coatings was improved by 15% after adding 0.2 wt.% nano ceria, which is attributed to the low content of spinel $NiCr_2O_4$ and high content of Cr_2O_3 in the thermal cycling, the refined and compact microstructure, and increased interfacial boundary.

Keywords high-velocity oxyfuel, nano ceria, NiCrAlY, ultrasonic gas atomization

1. Introduction

MCrAlY coatings are widely used to protect components of gas turbines and aero engines against high temperature degradation due to their excellent high-temperature oxidation and corrosion resistance, similar coefficient of thermal expansion (CTE) with the substrate and relatively good mechanical properties (Ref 1). The coatings can be used as either single overlay coating to promote high temperature oxidation resistance of substrates or bond coat for thermal barrier coatings (TBCs) to decrease the inter-laminar stress between ceramic top coat and substrate.

As an important protective coating at elevated temperature, MCrAlY coatings was applied for turbine engines over two decades ago, but its premature failure during thermal cycling is still a critical problem, which limits the lifetime of the coated components (Ref 2). So, great attentions have been focused on improving their high temperature properties such as thermal shock resistance and oxidation resistance (Ref 3-7).

Ceria has been proved effective for optimizing the mechanical properties and corrosion resistance of coating due to its unique properties (Ref 8, 9). One of our authors, You Wang (Ref 10-13), firstly introduced ceria to improve wear and corrosion of coatings. Jayaganthan et al. (Ref 8, 14-16) recently did meaningful work on the corrosion behavior of NiCrAlY + 0.4 wt.% CeO_2 coatings. In recent years, there has been a great scientific interest in the study of nano ceria due to its distinctive characteristics and novel options for a wide range of applications (Ref 17). The fine particle of nano ceria exhibits unique UV absorbing ability, high stability at high temperatures, and high hardness (Ref 18, 19). To the best of authors' knowledge, no attention was paid to the researches on nano ceria modified MCrAlY coatings.

The present work aims to investigate the thermal shock behavior of NiCrAlY coatings without and with nano ceria and clarify the effect of nano ceria on the thermal shock resistance of NiCrAlY coatings. The results could be helpful on developing the high temperature protective coatings.

2. Experimental Procedure

5Cr21Mn9Ni4N heat-resistant steel was used as substrate. Nano ceria and pure metals of Cr, Al, Y, and Ni were used as raw materials of the coatings. The nominal composition of NiCrAlY (with nano ceria) coatings is 25.3 wt.% Cr, 10.3 wt.% Al, 1.1 wt.% Y, (0.2 wt.% nano ceria), and balance Ni. The sprayable powders were prepared by induction melting and ultrasonic gas atomization method. The parameters for ultrasonic gas atomization are shown in Table 1. Before coating deposition, the substrates were cleaned in acetone for 5 min and grit blasted using alumina with particles size of 20 mesh to remove surface oxides and obtain a rough surface. NiCrAlY coatings without and with nano ceria were deposited by high velocity oxygen fuel (HVOF) spraying

Xiaoguang Sun, Department of Materials Science, Harbin Institute of Technology, Harbin 150001, China and Department of Chemical and Materials Engineering, University of Alberta, Edmonton T6G 2V4, Canada; **Shufen Chen, You Wang, Zhaoyi Pan,** and **Liang Wang**, Department of Materials Science, Harbin Institute of Technology, Harbin 150001, China. Contact e-mails: wangyou@hit.edu.cn.

technique (DJ 2700, Sulzer Metco). The spraying parameters are listed in Table 2.

The morphology and chemical composition of powders and coatings of NiCrAlY without and with nano ceria were examined by a scanning electron microscopy (SEM, FEI, QuanTA-200) equipped with an energy dispersive spectrometer (EDS). The particle size distribution of powders was measured by a particle size analyzer. The flowability was measured using a Hall Flowmeter (HYL-102, Hengyu). The phase compositions of coatings were detected by x-ray diffraction (XRD, Rigaku, D/MAX2400). The surface roughness of the as-sprayed coatings was measured by a surface profiler (Taylor Honson, S4C-3D).

The microhardness was measured with a Vickers indenter under a load of 100 g for 10 s. The adhesive strength of coatings was tested according to the ASTM C633-01 standard.

Thermal shock tests were conducted with a muffle furnace at 1000 °C in static air. Each cycle consisted of 5 min immersion in the furnace followed by quenching in water of 20 °C. The thermal shock cycles corresponding to spallation of 10% surface area of the coatings were defined as the lifetime. Three samples were tested in the identical condition to obtain the average value of cyclic oxidation life of the coating.

Table 1 Parameters of ultrasonic gas atomization

Parameters	Details
Vacuum of melting, Pa	3.5×10^{-3}
Atomizing medium	Ar
Atomizing pressure, MPa	11
Transducer frequency, KHz	50
Transducer amplitude, μm	50
Atomizing temperature, °C	1200
Inner diameter of nozzle, mm	Φ3.2

Table 2 Parameters of HVOF spraying

Parameters	Details
Fuel pressure (C_3H_8, psi)	85
Oxygen pressure, psi	150
Air pressure, psi	110
Feed rate, g/min	42
Flow rate of carrier gas, L/min	9
Spray distance, mm	240

3. Results and Discussion

3.1 Morphology of the As-Atomized Powders

Figure 1 shows the SEM images and particle size distribution of the NiCrAlY powders without and with

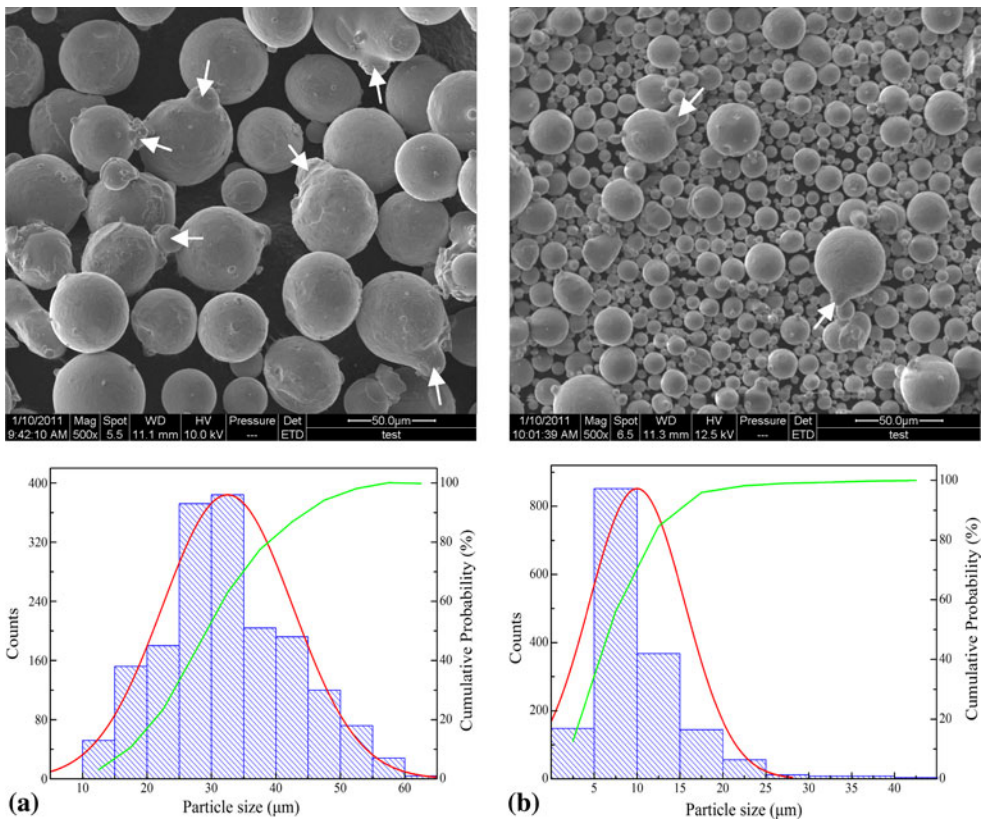

Fig. 1 SEM images and particle size distribution of the NiCrAlY (a) and NiCrAlY-0.2 wt.% nano ceria (b) powders

0.2 wt.% nano ceria. Most of the powders have a spherical, smooth, and dense surface. But there are also powders with irregular shape because small particles with size below 10 μm agglomerate, as satellites, to the large ones with size around 40 μm during solidification. This phenomenon is much more visible for the NiCrAlY powders than that modified by nano ceria (as shown in white arrows), which is related to the particle size distribution. According to statistics, the size of 90% of the NiCrAlY powders ranges from 10 to 45 μm and the mean size is around 33.6 μm. However, the size of 90% of the NiCrAlY powders with nano ceria ranges from 5 to 15 μm and the mean size is around 10 μm, which means that the particle size is uniform and refined after adding minor nano ceria.

The nano ceria takes important role in the refinement of the powders. Cerium is a surface-active element and thus reduces the surface tension and the interfacial energy between the crystal nucleus and the melt during the process of solidification (Ref 20), and the reduction of surface energy prohibit the agglomeration of melt droplets.

There will be further reduction in the surface energy if two particles combine. As we know, the trend for a relatively big particle combining a small particle is much easier than that for two small particles because there will be bigger reduction in the surface energy for the former one. The particle size is refined and the size distribution is much narrow after adding nano ceria, so the amount of satellites decreases. Because the existence of satellites can affect the flowability of the powders, the flowability of the powder with nano ceria also increases, which was confirmed by the experimental results.

3.2 Microstructure and Mechanical Properties of the As-Sprayed Coatings

Figure 2 shows the surface and cross-section morphology of both as-sprayed coatings. It can be seen from Fig. 2(a) and (b), there are un-melted particles, pores, and grazed regions (indicating melting and re-solidification of powders during spraying) in the NiCrAlY coating. The coating is composed of numerous splats overlapping together.

After adding nano ceria, the number of un-melted particles was reduced drastically, the microstructure of coatings was refined and the coating surface was smoother. The small particles melt easier than bigger ones, which result in the reduction of un-melted particles and surface roughness. As is detected, the surface roughness *Ra* of the as-sprayed NiCrAlY coating without and with nano ceria is 9.5 and 7.6, respectively.

Moreover, the coating was more compact after adding nano ceria. There was much less micro-pores in the

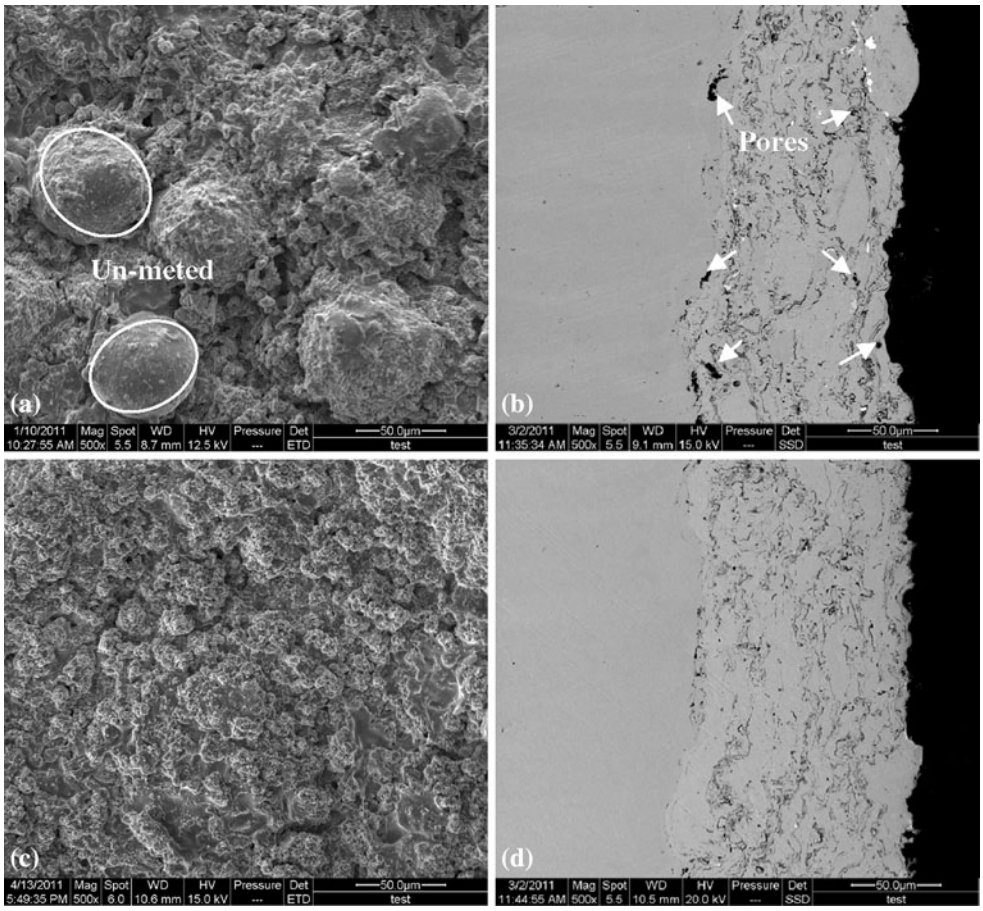

Fig. 2 Surface and cross-section morphology of the NiCrAlY (a and b) and NiCrAlY-0.2 wt.% nano ceria (c and d) coatings

NiCrAlY-0.2 wt.% nano ceria coating (Fig. 2c and d), which was also closely related to the reduction of un-melted particle. It is easier to produce space between un-melted particles that hard to be filled with melt.

A certain amount of oxides, which were observed as black contrast at the interface of lamellar structure, formed in both as-sprayed coatings. In HVOF spraying process, particles flying at high-speed impact on substrate or previously deposited coating layer and form typical lamellar structure. As HVOF spraying was performed in air, the scale-forming elements, such as Al and Cr showing high affinity with oxygen, in an in-flight molten particle easily react with the dissociated oxygen atom entrapped into the flame from environment. The oxidation behavior of the thermal spraying coating occurs in the following two processing: the in-flight melting powders and the particles impacting on substrate or previously sprayed coating layer. Moreover, spraying progress also affects the oxidation behavior of coatings. HVOF is characterized by shorter residence time in flame and higher kinetic energy of particles impacting, which is capable of depositing coatings with lower oxidation degree than many others thermal spraying technologies (Ref 21, 22).

Figure 3 shows the XRD patterns of both as-sprayed coatings. The main phases were composed of Ni_3Cr_2 and Ni_3Al for both coatings. A few α-Al_2O_3 was detected in the coating with nano ceria, which act as protective film produced in the spraying process. Nano ceria is surface-active and may adsorb oxygen from air easily. During HVOF spraying, the molten Al reacted easily with oxygen adsorbed on the surface of nano ceria particles and forms Al_2O_3.

Figure 4 shows the microhardness and adhesive strength of both coatings. Both the hardness and adhesive strength of the NiCrAlY-0.2 wt.% nano ceria coating are higher than that of NiCrAlY coating, which is due to the refinement of microstructure and the decrease of the defects, such as pores and oxides. The homogeneous and refined microstructure as well as the increased solubility of Cr of as-spayed coatings with nano ceria are responsible for the improvement of microhardness (Ref 7).

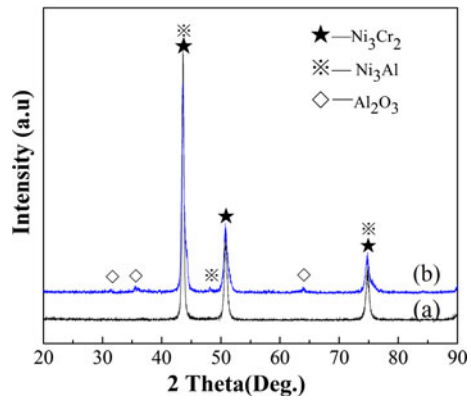

Fig. 3 XRD pattern of the as-sprayed NiCrAlY (a) and NiCrAlY-0.2 wt.% nano ceria (b) coatings

Adhesive strength is an important criterion to evaluate advanced coatings. The adhesive strength of NiCrAlY coatings deposited by HVOF technology is more than 50 MPa, while it only reaches about 30 MPa by plasma spraying. HVOF is characterized by depositing coating with residual compressive stress which is favorable for the adhesive strength of coating (Ref 21, 23). The compact microstructure between the coating and substrate is expected to be beneficial to the improvement of adhesive strength after adding nano ceria (Ref 24).

3.3 Thermal Shock Resistance at 1000 °C

The NiCrAlY and NiCrAlY-0.2 wt.% nano ceria coatings endured 85 and 98 cycles, respectively, before failure in thermal shock resistance test at 1000 °C. The thermal cycle life of NiCrAlY coatings is improved by 15% after adding 0.2 wt.% nano ceria. As is known, the oxidation resistance of coatings at elevated temperature is greatly influenced by the microstructure of as-sprayed coatings. Firstly, the boundary between splats plays an important role in the high resistance of coatings. The increase of the boundary can prohibit the inward diffusion of oxygen. The initial feedstock of the NiCrAlY coating with 0.2 wt.% nano ceria is refined, so the interfacial boundary between splats increases aftering depositing on the substrate and is useful to inhibit the inward diffusion of oxygen. In addition, the pores in the coating can easily become the penetration paths for oxygen, which accelerates internal oxidation of coatings (Ref 25). The NiCrAlY coating with 0.2 wt.% nano ceria has less pores and is more compact, this also contributes to the prolonged lifetime at high temperature.

The surface morphologies of both coatings after 85 cycles at 1000 °C are shown in Fig. 5. The coatings show different surface morphologies. Cracks are visible on the surface of NiCrAlY coating. And there is a great amount of spinel structure phase on the surface. According to the XRD analysis (Fig. 6), this phase is $NiCr_2O_4$, which is formed between NiO and Cr_2O_3 through a solid state

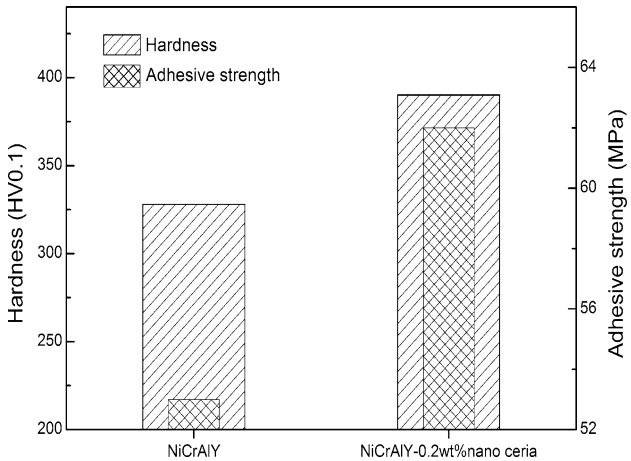

Fig. 4 The microhardness and adhesive strength of the NiCrAlY and NiCrAlY-0.2 wt.% nano ceria coatings

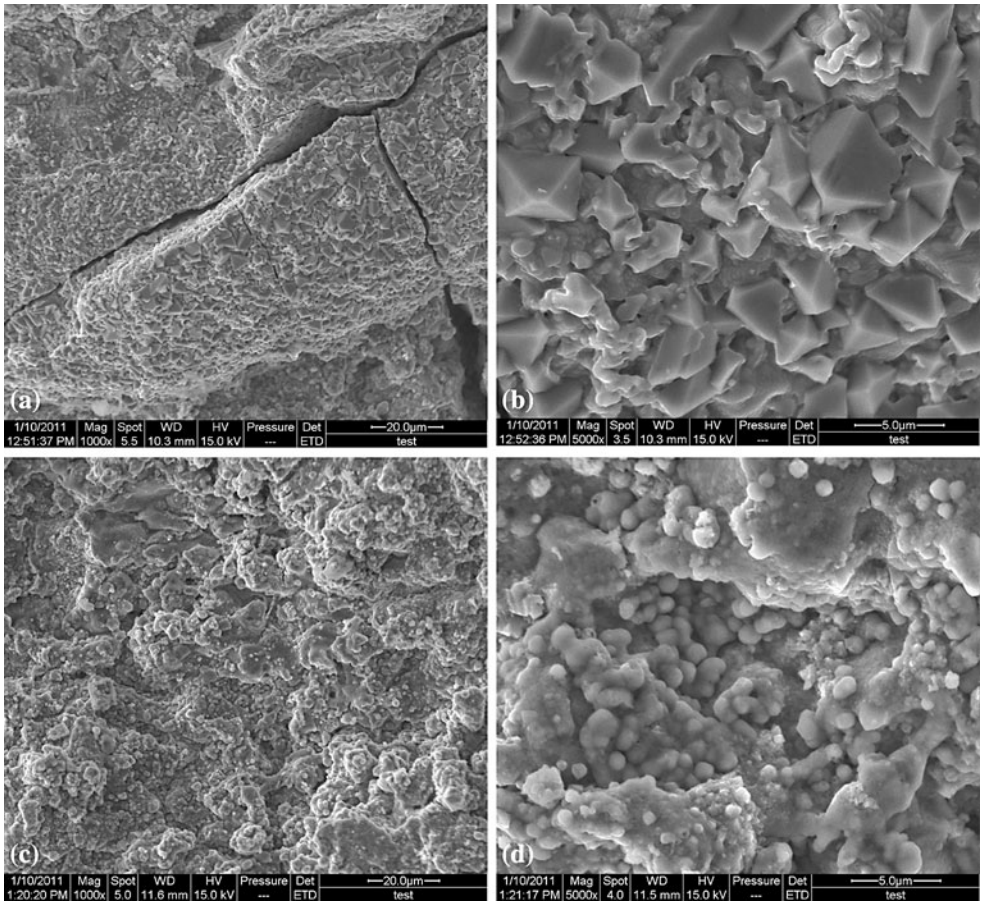

Fig. 5 Surface morphology of the NiCrAlY(a and b) and NiCrAlY-0.2 wt.% nano ceria (c and d) coatings after thermal shock for 85 cycles at 1000 °C

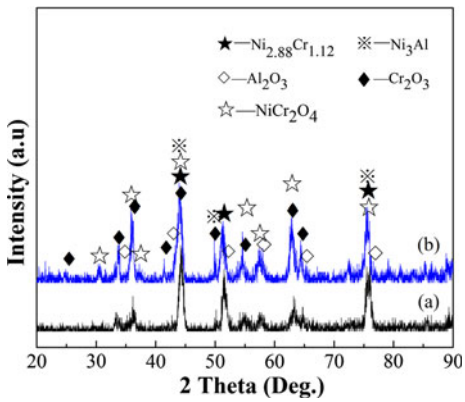

Fig. 6 XRD pattern of the NiCrAlY (a) and NiCrAlY-0.2 wt.% nano ceria (b) coatings after thermal shock for 85 cycles at 1000 °C

reaction during oxidation (Ref 26). After adding nano ceria, there is no visible crack even after experiencing the same thermal shock cycles with NiCrAlY coating. The morphology is characterized by spherical agglomeration, which is mainly composed of Cr_2O_3, confirmed by the XRD result. Although both coatings have $Ni_{2.88}Cr_{1.12}$, Ni_3Al, Al_2O_3, and $NiCr_2O_4$, the coating with nano ceria has high proportion of Cr_2O_3. Usually, Cr_2O_3 reacts with NiO and forms $NiCr_2O_4$ in NiCrAlY coatings under high temperature. $NiCr_2O_4$ is protective in hot corrosion environment, but it is a brittle phase and easily cracks in a thermal cycling process. Cr_2O_3 is thermodynamically stable at temperatures higher than 500 °C (Ref 27). It is isostructural with sapphire (Al_2O_3) and has desirable mechanical and chemical properties, such as high hardness, chemical inertness, and high-temperature stability (Ref 28, 29). The increase of Cr_2O_3 in the NiCrAlY-0.2 wt.% nano ceria coating indicates that the formation of spinel $NiCr_2O_4$ is inhibited, which can prolong the lifetime of the coating by restraining the origination and propagation of crack under thermal shock process.

The cross section morphology and elements distribution of both coatings after thermal shock for 85 cycles at 1000 °C are shown in Fig. 7. The elements distribution indicates that Al and O concentrated on the interface between coating and substrate, which easily result in the spalling of the coating from the substrate in thermal cycling process. However, there is a net-like distribution of Cr, Al, and O in the coating with 0.2 wt.% nano ceria, which is beneficial to the bonding between coating and the substrate and maintain the integration of the coating. The

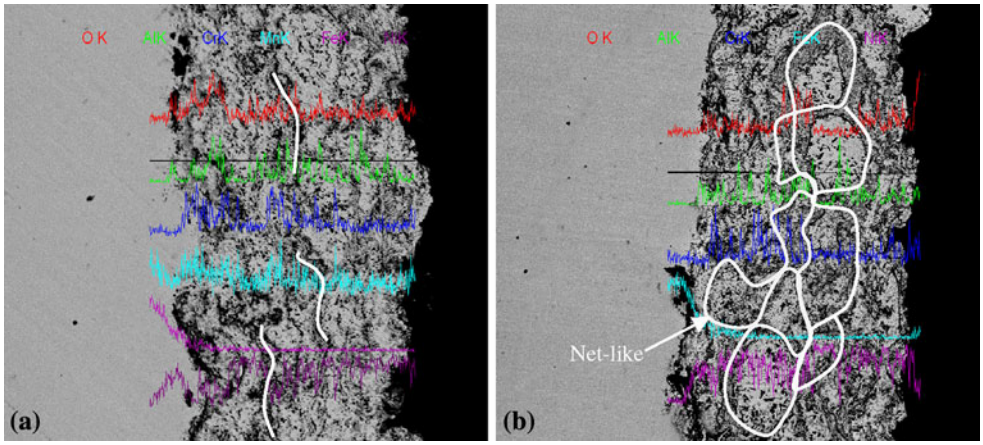

Fig.7 Cross section morphology and elements distribution of the NiCrAlY (a) and NiCrAlY-0.2 wt.% nano ceria (b) coatings after thermal shock for 85 cycles at 1000 °C

diffusion of Al, Cr from coating to substrate could hardly be seen in both coatings, which is beneficial for prolonging the lifetime. At 1000 °C, Al_2O_3 is more easily formed in coating due to its greater formation Gibbs energy than that of Cr_2O_3 (−1270.5 KJ/mol Al_2O_3 and −803.0 KJ/mol Cr_2O_3). But the content of Al is less than that of Cr. After 85 thermal cycles, there is less available Al to form Al_2O_3. Once the Al_2O_3 film is damaged, Cr_2O_3 will form as soon as possible when oxygen atoms in atmosphere penetrating into the coatings, which can hinder further penetration of oxygen and improve the thermal shock resistance of coating. So, the significantly improved thermal cycle life of NiCrAlY-0.2 wt.% nano ceria confirmed that Cr_2O_3, to some extent, can prolong the lifetime of NiCrAlY coatings under thermal cycling.

4. Conclusions

In this paper, effects of nano ceria on microstructure, mechanical properties, and thermal shock resistance of NiCrAlY coatings were investigated. Some useful conclusion was obtained. Because the high surface-active nano ceria reduced the surface tension of the melt and prohibited the agglomeration of melt droplets, the particle size of NiCrAlY powders was uniform and refined. There content of satellite particles in the powders decreased, which increased the flowability of the powders. In the as-sprayed coatings, the number of un-melted particles was reduced drastically, the microstructure was refined and compact and the coating surface was also smoother due to the refinement of sprayable powders. Both the hardness and adhesive strength of the NiCrAlY increased due to the refinement of microstructure and the decrease of the defects, such as pores and oxides, after adding nano ceria. The thermal cycle life of NiCrAlY coatings was improved by 15% after adding 0.2 wt.% nano ceria. In the thermal cycling, the content of spinel $NiCr_2O_4$ was low and that of Cr_2O_3 was high, which contributed to the improvement of thermal shock resistance. The refined and compact microstructure and increased interfacial boundary also played important role in the high thermal shock resistance.

Acknowledgment

This work was supported by Program of Excellent Team at Harbin Institute of Technology. The authors would like to thank Dr. Wanliang Hou from Institute of Metal Research, Chinese Academy of Sciences for his support on powder preparation.

References

1. A.G. Evans, D.R. Mumm, J.W. Hutchinson, G.H. Meier, and F.S. Pettit, Mechanisms Controlling the Durability of Thermal Barrier Coatings, *Prog. Mater. Sci.*, 2001, **46**, p 505-553
2. L. Ajdelsztajn, F. Tang, J. Schoenung, G. Kim, and V. Provenzano, Synthesis and Oxidation Behavior of Nanocrystalline MCrAlY Bond Coatings, *J. Therm. Spray Technol.*, 2005, **14**(1), p 23-30
3. M. Schütze, M. Malessa, V. Rohr, and T. Weber, Development of Coatings for Protection in Specific High Temperature Environments, *Surf. Coat. Technol.*, 2006, **201**(7), p 3872-3879
4. N.J. Simms, A. Encinas-Oropesa, and J.R. Nicholls, Hot Corrosion of Coated and Uncoated Single Crystal Gas Turbine Materials, *Mater. Corros.*, 2008, **59**(6), p 476-483
5. Y. Wang, W. Tian, and Y. Yang, Thermal Shock Behavior of Nanostructured and Conventional Al_2O_3/13 wt% TiO_2 Coatings Fabricated by Plasma Spraying, *Surf. Coat. Technol.*, 2007, **201**(18), p 7746-7754
6. A. Fossati, M. Di Ferdinando, A. Lavacchi, U. Bardi, C. Giolli, and A. Scrivani, Improvement of the Isothermal Oxidation Resistance of CoNiCrAlY Coating Sprayed by High Velocity Oxygen Fuel, *Surf. Coat. Technol.*, 2010, **204**(21-22), p 3723-3728
7. M. Di Ferdinando, A. Fossati, A. Lavacchi, U. Bardi, F. Borgioli, C. Borri, C. Giolli, and A. Scrivani, Isothermal Oxidation Resistance Comparison Between Air Plasma Sprayed, Vacuum Plasma Sprayed and High Velocity Oxygen Fuel Sprayed CoNiCrAlY Bond Coats, *Surf. Coat. Technol.*, 2010, **204**(15), p 2499-2503
8. S. Kamal, R. Jayaganthan, and S. Prakash, Mechanical and Microstructural Characteristics of Detonation Gun Sprayed NiCrAlY + 0.4 wt% CeO_2 Coatings on Superalloys, *Mater. Chem. Phys.*, 2010, **122**(1), p 262-268
9. Y. Wang, X.G. Sun, J.Q. He, S.F. Chen, L. Wang, and Z. Wang, High Temperature Sulphidation of HVOF Sprayed CeO_2

Modified NiCrAlY Coatings in H_2/H_2S Atmospheres, *Surf. Eng.*, 2011. http://dx.doi.org/10.1179/1743294411Y.0000000050
10. Y. Wang, J. Liu, Z. Yu, G. Wang, and Q. Li, Influence of CeO_2 on Micro-Structure and Wear Resistance of M80S20 Laser-Alloyed Layer, *Chin. J. Lasers*, 1992, **10**(12), p 777-780
11. Y. Wang, J.J. Liu, and Z.H. Yu, Effect of Rare Earth Elements on Microstructure and Wear Resistance of Laser Remelted Iron Alloy Coatings Containing Metalloids, *Surf. Eng.*, 1993, **9**(2), p 151-153
12. Y. Wang, Y. Yang, and M.F. Yan, Microstructures, Hardness and Erosion Behavior of Thermal Sprayed and Heat Treated NiAl Coatings with Different Ceria, *Wear*, 2007, **263**(1-6), p 371-378
13. Y. Wang, Z. Wang, Y. Yang, and W. Chen, The Effects of Ceria on the Mechanical Properties and Thermal Shock Resistance of Thermal Sprayed NiAl Intermetallic Coatings, *Intermetallics*, 2008, **16**(5), p 682-688
14. S. Kamal, R. Jayaganthan, and S. Prakash, Hot Corrosion Studies of Detonation-Gun-Sprayed NiCrAlY + 0.4 wt.% CeO_2 Coated Superalloys in Molten Salt Environment, *J. Mater. Eng. Perform.*, 2011, **20**(6), p 1068-1077
15. R.A. Mahesh, R. Jayaganthan, and S. Prakash, A Study on the Oxidation Behavior of HVOF Sprayed NiCrAlY-0.4 wt.% CeO_2 Coatings on Superalloys at Elevated Temperature, *Mater. Chem. Phys.*, 2010, **119**(3), p 449-457
16. R.A. Mahesh, R. Jayaganthan, and S. Prakash, Characterisation of HVOF Sprayed NiCrAlY-0.4 wt% CeO_2 Coatings on Superalloys, *Surf. Eng.*, 2008, **24**(5), p 366-373
17. M.G. Sujana, K.K. Chattopadyay, and S. Anand, Characterization and Optical Properties of Nano-Ceria Synthesized by Surfactant-Mediated Precipitation Technique in Mixed Solvent System, *Appl. Surf. Sci.*, 2008, **254**(22), p 7405-7409
18. T. Ming-Shyong, Powder Synthesis of Nano Grade Cerium Oxide via Homogenous Precipitation and Its Polishing Performance, *Mater. Sci. Eng. B*, 2004, **110**(2), p 132-134
19. J.-S. Lee and S.-C. Choi, Crystallization Behavior of Nano-Ceria Powders by Hydrothermal Synthesis Using a Mixture of H_2O_2 and NH_4OH, *Mater. Lett.*, 2004, **58**(3-4), p 390-393
20. Y.S. Tian, C.Z. Chen, L.X. Chen, and Q.H. Huo, Effect of RE Oxides on the Microstructure of the Coatings Fabricated on Titanium Alloys by Laser Alloying Technique, *Scr. Mater.*, 2006, **54**(5), p 847-852
21. F. Tang, Characterization of Oxide Scales Formed on HVOF NiCrAlY Coatings with Various Oxygen Contents Introduced During Thermal Spraying, *Scr. Mater.*, 2004, **51**(1), p 25-29
22. E. Lugscheider, C. Herbst, and L. Zhao, Parameter Studies on High-Velocity Oxy-Fuel Spraying of MCrAlY Coatings, *Surf. Coat. Technol.*, 1998, **108-109**, p 16-23
23. K. Nakamura, T. Kawabata, and Y. Mori, Size Distribution Analysis of Colloidal Gold by Small Angle X-ray Scattering and Light Absorbance, *Powder Technol.*, 2003, **131**(2-3), p 120-128
24. R.A. Mahesh, R. Jayaganthan, and S. Prakash, A Study on the Oxidation Behavior of HVOF Sprayed NiCrAlY-0.4 wt.% CeO_2 Coatings on Superalloys at Elevated Temperature, *Mater. Chem. Phys.*, 2010, **119**, p 49-457
25. H. Choi, B. Yoon, Kim. Hyungjun, and C. Leea, Isothermal Oxidation of Air Plasma Spray NiCrAlY Bond Coatings, *Surf. Coat. Technol.*, 2002, **105**, p 297-308
26. G.Y. Liang, C. Zhu, X.Y. Wu, and Y. Wu, The Formation Model of Ni-Cr Oxides on NiCoCrAlY-Sprayed Coating, *Appl. Surf. Sci.*, 2011, **257**(15), p 6468-6473
27. J. Wang, A. Gupta, and T.M. Klein, Plasma Enhanced Chemical Vapor Deposition of Cr_2O_3 Thin Films Using Chromium Hexacarbonyl ($Cr(CO)_6$) Precursor, *Thin Solid Films*, 2008, **516**(21), p 7366-7372
28. P. Schmuki, From Bacon to Barriers: A Review on the Passivity of Metals and Alloys, *J. Solid State Electrochem.*, 2002, **6**(3), p 145-164
29. K.P. Lillerud and P. Kofstad, On High Temperature Oxidation of Chromium—1. Oxidation of Annealed, Thermally Etched Chromium at 800 °C-1100 °C, *J. Electrochem. Soc.*, 1980, **127**(11), p 2397-2409